molecular pharmaceutics

Article

pubs.acs.org/molecularpharmaceutics

# Cationic PAMAM Dendrimers Disrupt Key Platelet Functions

Clinton F. Jones,[†] Robert A. Campbell,[‡] Zechariah Franks,[‡] Christopher C. Gibson,[‡,∥] Giridhar Thiagarajan,[§,∥] Adriana Vieira-de-Abreu,[‡,⊥] Sivaprasad Sukavaneshvar,[#] S. Fazal Mohammad,[#,▽,○] Dean Y. Li,[‡,◆,¶] Hamidreza Ghandehari,[†,§,∥] Andrew S. Weyrich,[‡,△] Benjamin D. Brooks,[†] and David W. Grainger*[,†,§,∥]

[†]Department of Pharmaceutics and Pharmaceutical Chemistry, Health Sciences, University of Utah, Salt Lake City, Utah 84112, United States

[‡]Program in Molecular Medicine, University of Utah School of Medicine, Salt Lake City, Utah 84132, United States

[§]Utah Center for Nanomedicine, Nano Institute of Utah, University of Utah, Salt Lake City, Utah 84108, United States

[∥]Department of Bioengineering, University of Utah, Salt Lake City, Utah 84112, United States

[⊥]Laboratório de Imunofarmacologia, Instituto Oswaldo Cruz, Fiocruz, Rio de Janeiro, Brazil

[#]Thrombodyne, Inc., Salt Lake City, Utah 84103, United States

[▽]Department of Pathology, University of Utah, Salt Lake City, Utah 84132, United States

[○]Utah Artificial Heart Institute, University of Utah, Salt Lake City, Utah 84112, United States

[◆]Division of Cardiology, Department of Internal Medicine, University of Utah, Salt Lake City, Utah 84132, United States

[¶]Department of Oncological Sciences, University of Utah, Salt Lake City, Utah 84132, United States

[△]Divisions of Pulmonary and Critical Care Medicine, Department of Internal Medicine, University of Utah, Salt Lake City, Utah 84132, United States

Supporting Information

**ABSTRACT:** Poly(amidoamine) (PAMAM) dendrimers have been proposed for a variety of biomedical applications and are increasingly studied as model nanomaterials for such use. The dendritic structure features both modular synthetic control of molecular size and shape and presentation of multiple equivalent terminal groups. These properties make PAMAM dendrimers highly functionalizable, versatile single-molecule nanoparticles with a high degree of consistency and low polydispersity. Recent nanotoxicological studies showed that intravenous administration of amine-terminated PAMAM dendrimers to mice was lethal, causing a disseminated intravascular coagulation-like condition. To elucidate the mechanisms underlying this coagulopathy, *in vitro* assessments of platelet functions in contact with PAMAM dendrimers were undertaken. This study demonstrates that cationic G7 PAMAM dendrimers activate platelets and dramatically alter their morphology. These changes to platelet morphology and activation state substantially altered platelet function, including increased aggregation and adherence to surfaces. Surprisingly, dendrimer exposure also attenuated platelet-dependent thrombin generation, indicating that not all platelet functions remained intact. These findings provide additional insight into PAMAM dendrimer effects on blood components and underscore the necessity for further research on the effects and mechanisms of PAMAM-specific and general nanoparticle toxicity in blood.

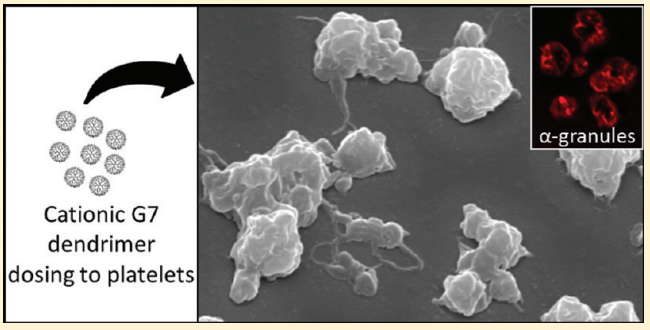


**KEYWORDS:** *nanotoxicity, PAMAM dendrimers, platelet activation, biocompatibility, thrombin generation*

## INTRODUCTION

Dendrimers are a specialized subclass of hyperbranched polymers, produced from stepwise synthetic strategies that yield well-defined, monodisperse molecular structures. Their unique molecular structure features characteristic repeated chemical units, each with multiple equivalent terminal groups, that, through repeated end group protection and condensation chemistries, yield multifunctional, single-molecule nanoparticles with a high degree of structural and chemical consistency, defined surface chemistry, and low polydispersity.[1] Different generations of dendrimers produce different sizes and densities

**Received:** November 27, 2011
**Revised:** March 31, 2012
**Accepted:** April 12, 2012
**Published:** April 12, 2012



  

of terminal functional groups, each with distinct properties. With diverse technological potential, some dendrimer chemistries are proposed for a variety of pharmaceutical applications, including cell transfection,[2,3] bioimaging,[4] and drug delivery.[5−10] In particular, dendrimers receive increasing attention for drug delivery in two distinct approaches: (1) as a platform for conjugated drug molecules, especially in cancer therapeutics,[6,11−15] and (2) as an encapsulating mechanism to improve drug solubility.[16,17]

Presently, the most direct route for drug administration is via the circulatory system (i.e., intravenous) because blood-borne active compounds reach tissue targets and less-accessible sites in short times via vascular transport. However, a major problem with this strategy is that blood proteins (~70 mg/mL in plasma) and cells (40−45% packed cell volume in blood) interact, bind, and complex with polymers and nanoparticles, often interfering with drug transport, targeting, clearance, and bioavailability.[18] Dendrimers are no exception; the ubiquitous binding of dendrimers and dendritically captured drugs to blood cells, platelets, plasma proteins, and the vascular endothelium will certainly affect drug efficacy.[19] Significantly, undesired or uncontrolled dendrimer interactions with blood components and host tissues can readily produce serious toxicity.[20−23]

Cationic (amine-terminated) polyamidoamine (PAMAM) dendrimers have been shown *in vitro* to destabilize erythrocyte membranes,[24] potentially inducing hemolysis in a manner that is both dose- and generation-dependent.[17,25] Other studies have also shown that high-generation PAMAM dendrimers induce membrane composition-specific alterations in anionic lipid vesicle morphology.[19,26] However, of greatest concern are murine experiments involving injections of high-generation PAMAM dendrimers (G7-$NH_2$) that resulted in hemolysis and catastrophic coagulopathy,[27] and also a very recent *in vitro* study showing size- and surface charge-dependence of PAMAM dendrimer-induced platelet aggregation.[28] For validating any *in vivo* application, careful assessment of dendrimer toxicities and biological interactions are essential, especially as injected, systemically bioavailable drugs and drug carriers. Currently, dendrimer toxicity remains relatively uncharacterized,[19,25,29−33] particularly in the specific and essential case of hematologic toxicity. Understanding specific relationships between dendrimer size and chemistry and their blood interactions and biodistributions would enable the required predictive models for assessing possible human toxicities[34] and, importantly, inform structure−property relationships for improving rational designs for *in vivo* use.

Platelets are anucleate, 2−3 $\mu$m diameter, cytoplasmic discs—the smallest formed membranous element in blood. They comprise a major metabolically active blood component, circulating constantly at ~$2.5 \times 10^8$ platelets/mL of blood, are highly responsive to diverse physical and biochemical stimuli with potent coagulation and growth factors, and are responsible primarily for hemostasis. Until recently, platelets have not received significant research attention regarding possible mechanisms of nanoparticle toxicity. However, platelet activation by injected drug delivery nanoconstructs could readily result in unintended—even fatal—consequences in host circulation. This potential was recently demonstrated for PAMAM dendrimers injected into systemic blood circulation in mice.[27,28] Additional mechanistic information on platelet activation and dendrimer−platelet interactions that produce these problems is required to both avoid undesired dendrimer toxicities in blood and guide dendrimer designs to avoid these issues.

In this study, we compare cationic, anionic, and polar uncharged (e.g., -$NH_2$, -COOH, and -OH terminated) high-generation dendrimer effects on *in vitro* platelet morphology, activation states, and hemostatic functions. Data shown for PAMAM dendrimer−platelet reactivity compliment recently published related data suggesting that cationic PAMAM dendrimers cause platelet activation and aggregation[28] by further elucidating mechanisms by which higher generation (G7), more densely cationic PAMAM dendrimers affect platelet morphology and functions in blood.

## MATERIALS AND METHODS

**Preparation and Characterization of FITC-Labeled PAMAM Dendrimers.** G6.5-COOH, G7-OH, and G7-$NH_2$ PAMAM dendrimers with an ethylenediamine core were purchased from Sigma Aldrich (St. Louis, MO) and fractionated on a preparative size exclusion column (SEC, Sephadex Hiload 75, GE Healthcare, Piscataway, NJ) to remove low-molecular-weight oligomers. Characterization of the native dendrimers has been reported previously.[27] PAMAM dendrimers were labeled with fluorescein isothiocyanate (FITC) (for G7-$NH_2$ and G7-OH dendrimers) or 5-(aminomethyl)-fluorescein (for G6.5-COOH dendrimers), as reported previously.[35] Briefly, G7-OH (12.8 $\mu$M) and FITC (25.6 $\mu$M) (Sigma Aldrich, USA) were reacted in a molar ratio of 1:2 with a molar equivalent of triethylamine (Sigma-Alrich, USA) in DMSO for 72 h under a steady stream of nitrogen gas. G7-$NH_2$ (12.8 $\mu$M) and FITC (25.6 $\mu$M) were each dissolved in DMSO and conjugated overnight in nitrogen atmosphere at room temperature with feed molar ratios of 1:2. G6.5-COOH (13 $\mu$M) dissolved in DMSO and carboxyl groups were activated using NHS/EDC reagents (Sigma-Alrich, USA) at the molar ratio 1:4. Subsequently, 5-(aminomethyl)fluorescein (25 $\mu$M in DMSO) (Sigma-Aldrich, USA) was added to this mixture and allowed to react overnight under nitrogen at the molar ratio 1:2 (Supporting Information Scheme 1). Fluorescently labeled PAMAM dendrimers were dialyzed against deionized water using 500 Da molecular-weight-cutoff membranes (Spectrum Laboratories, Inc., Rancho Dominguez, USA) and subsequently fractionated on a preparative Sephadex Hiload 75 size exclusion column (SEC, GE Healthcare, Piscataway, NJ) to remove residual, free FITC, and other small molecular weight impurities. Fractionated PAMAM dendrimers were dialyzed again and lyophilized. Purified FITC-labeled PAMAM dendrimers were then characterized at unbuffered, neutral pH as previously described for the unlabeled dendrimers.[27] Zeta potential was measured using a Malvern Zetasizer NanoZS (Malvern, U.K.), particle size was verified against unlabeled dendrimer size by SEC on an analytical Superose 6 10/300 GL column (GE Healthcare, Piscataway, USA) with an elution buffer of PBS/acetonitrile (80:20) with 0.1% sodium azide, and dye labeling densities were determined at neutral pH by optical absorbance (495 nm) compared to free FITC standards and background-subtracted unlabeled dendrimer absorbance on a Cary 400 Bio UV−vis spectrophotometer (Varian, Palo Alto, CA) at ambient temperature (Supporting Information Figure 1).

**Whole Blood Collection and Plasma Preparation.** The University of Utah Institutional Review Board approved this study, and all subjects provided informed consent. Human peripheral venous blood (25−50 mL) from healthy, medi-

cation-free adult subjects was drawn into acid-citrate-dextrose (1.4 mL of ACD/8.6 mL of blood) through a standard venipuncture technique and used immediately upon collection. Plasma was harvested by centrifuging whole blood at 500*g* for 20 min and then once more at 13,000*g* for 2 min to remove any remaining cell contaminants.

**Platelet Isolation.** Human platelets were isolated from whole blood and suspended in M199 medium (Lonza, Walkersville, USA) ($1 \times 10^8$ platelets/mL, final) as previously described.[36−38] Previous work has demonstrated that leukocyte contamination is minimal in platelet isolates obtained by this protocol.[38,39]

**Thrombin Generation Assays.** Whole blood was treated with saline controls or dendrimers for either 30 min or 4 h at 37 °C. Platelet-rich plasma (PRP) was isolated by centrifuging whole blood for 20 min at 150*g*. In some experiments, PRP was isolated before addition of agonist and treated for 30 min or 4 h. Additional $CaCl_2$ was added to the substrate reagent to reach a final concentration of 15 mM $CaCl_2$. Reagents were combined with sample plasma in duplicate according to manufacturer's instructions in a 96-well plate and read every minute for 90 min. Thrombin generation was measured with a Synergy HT multi Detection Microplate Reader (Bio-Tek Instruments, Winooski, USA) at an excitation/emission wavelength of 360 nm/460 nm. Thrombin calibration curves were performed and analyzed according to manufacturer's instructions. Falcon PRO-BIND 96-well flat bottom plates (Becton Dickinson, Franklin Lakes, USA) were used to perform the fluorogenic reactions. Fluorogenic substrate (Z-Gly-Gly-Arg-AMC; 0.5 mM, final), and RC high reagent (7.16 pM TF and 0.32 $\mu$M phospholipid micelles, final) were purchased from Technoclone (Vienna, Austria).

**Immunoassays and Flow Cytometry.** Platelets resuspended in M199 were treated with dendrimer or thrombin at indicated concentrations and for indicated times and centrifuged at 13000*g* for 2 min to harvest cell-free supernatants. Regulated on Activation Normal T-Expressed and Secreted (RANTES) and Platelet Factor 4 (PF4) were measured using ELISA (R&D Systems, Minneapolis, MN).[40,41] In separate experiments, platelets treated with FITC-labeled dendrimers for indicated times were stained with antihuman P-selectin (CD62) phycoerythrin (PE) (BD Biosciences, San Jose, CA). Platelets were analyzed by flow cytometry using a FACScalibur (BD Biosciences, USA). Experiments were conducted and analyzed in biological triplicate.

**Confocal Microscopy.** Freshly isolated platelets were fixed either immediately to assess baseline morphology or after 30-min treatment with human thrombin (0.1 U/mL, final) (Sigma-Aldrich) or FITC-labeled dendrimers (100 $\mu$g/mL final). At the end of each experimental period, buffered paraformaldehyde (2% final) was added directly to the washed platelets as previously described to maintain the native cell morphology. Fixed platelets (10,000 total for each sample) were subsequently layered onto Vectabond-coated coverslips (Vector Laboratories, USA) using a cytospin centrifuge (Shandon Cytospin; Thermo Fisher Scientific, USA). Wheat germ agglutinin (WGA, Alexa 555-labeled, Invitrogen, Carlsbad, USA) was used as a counterstain to stain granules and membranes of platelets.[42] Fluorescence microscopy and high-resolution confocal reflection microscopy was performed using an Olympus Fluoview FV1000 confocal-scanning microscope equipped with a 60×/1.42 NA oil objective for viewing platelets. An Olympus FVS-PSU/IX2-UCB camera and scanning unit and Olympus Fluoview and FV1000 image acquisition software (version 5.0) were used for recording.

**Platelet Aggregometry.** Dendrimers were added to citrated human whole blood or PRP to a final concentration of 100 $\mu$g/mL, and aggregation in whole blood was then measured by impedance in a whole blood aggregometer (model 592, Chronolog, Havertown, PA) or by turbidity in a light transmission aggregometer (model 560CA, Chronolog, Havertown, USA) immediately after addition of dendrimer or agonist. ADP (10 $\mu$M final, Sigma Aldrich, St. Louis, MO) was used as a positive control.

**Scanning Electron Microscopy (SEM).** PRP was treated with dendrimers (100 $\mu$g/mL, final) or thrombin (0.1 U/mL, final) for 45 min at room temperature. The PRP was then diluted 1:20 with Karnovsky's fixative. A small aliquot of each platelet treatment was pipetted onto glass coverslips, and the platelets were allowed to settle to the glass surface for 30 min before dehydration proceeded on the coverslip by graded ethanol solutions. Coverslips were mounted on SEM stubs, sputtered with gold for 5 min, and imaged using a JEOL CarryScope (JCM-5700). Images were taken at 2500× with a 34−55 mm working distance and a 20 kV accelerating voltage.

**Platelet Shear-flow Adhesion Assay.** Platelet interaction with adsorbed fibrinogen was assayed under controlled shear conditions using a parallel plate flow chamber (Ibidi 0.4 VI $\mu$-plates, Ibidi GmbH, Germany) with six independent wells on a standard microscope slide-sized plate. Each well was coated with 0.5 mg/mL human fibrinogen at 37 °C for at least 30 min for monolayer adsorption. Platelets were fluorescently prelabeled by incubating with 1 $\mu$M CellTracker Orange CMRA (Invitrogen) for 1 h followed by a wash step. In some experiments, platelets were also treated with abciximab (0.136 $\mu$M final, University of Utah Pharmacy) for 30 min before treatment with the designated agonist. Immediately prior to platelet perfusion, the chamber was rinsed three times with PBS and mounted in a 37 °C humidified chamber (Okolab Via Campana, Italy) on an Olympus IX-81 epifluorescent microscope. Isolated platelets were treated with saline, thrombin (0.5 U/mL, final), or dendrimers (100 $\mu$g/mL, final). Thrombin-treated platelets were incubated for 5 min before perfusion, and saline- or G7-$NH_2$-treated platelets were immediately perfused through the flow chamber at a wall shear rate of 200 $s^{-1}$ (1.14 mL/min flow rate) using a Harvard Apparatus syringe pump (Holliston, USA). Real-time platelet adhesion to the bottom chamber surface was viewed with a 10× objective with mercury lamp illumination (100 W, 589/15 nm excitation, 640−675 emission), and images were captured at 1-s intervals for 360 s using an ORCA-ER monochrome CCD camera (Hamamatsu). The camera and shutters were controlled by Metamorph imaging software (version 7, Meta Imaging). All image processing and analysis were performed on image stacks in ImageJ software (National Institutes of Health, USA). Two subtraction methods were employed during image processing to remove unbound bulk platelet fluorescence and intrinsic camera field noise: fluorescence from unbound platelets was eliminated by its isolation (by sequence subtraction of an identical stack offset by one image, ImageJ image calculator function) and direct subtraction of the resulting isolated unbound platelet fluorescence image sequence (ImageJ image calculator function) from the original stack. Subsequently, image stacks were background-subtracted (50-pixel sliding parabaloid options) and thresholded (dark background option).

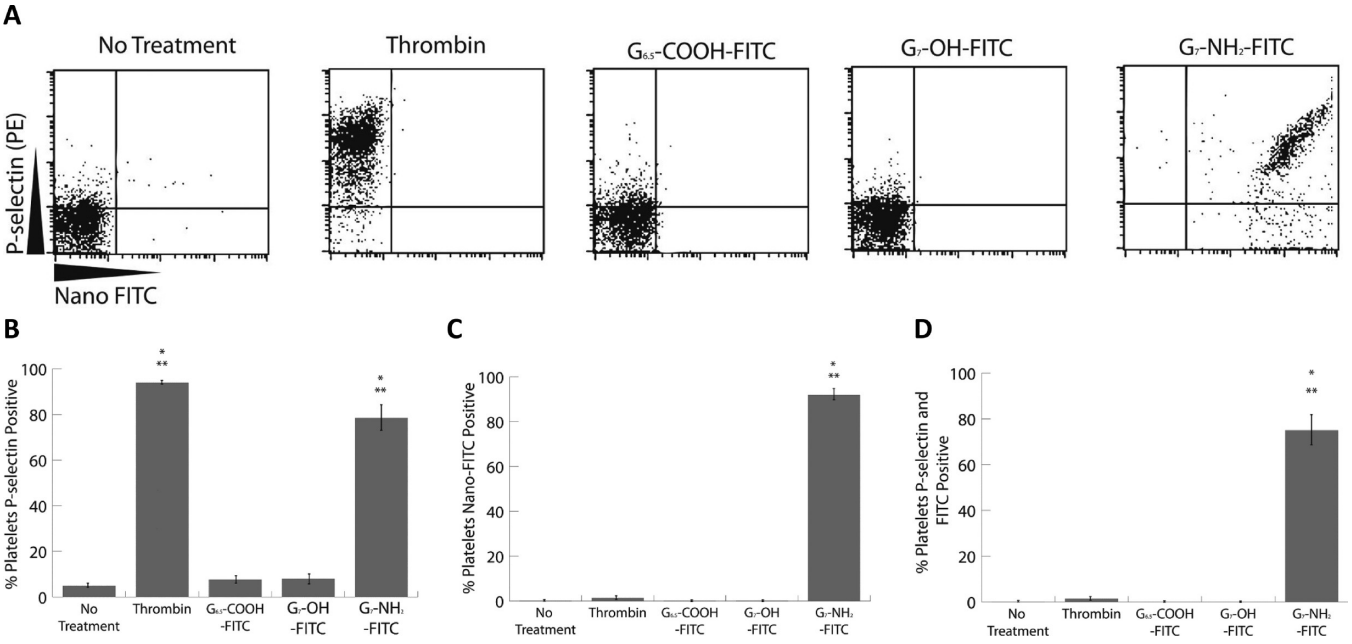


**Figure 1.** G7-$NH_2$-FITC dendrimers induce P-selectin expression on platelets (A–D). Platelets were treated with saline, thrombin, or 100 $\mu$g/mL of different functionalized dendrimers for 30 min. Thrombin induces P-selectin expression while the G6.5-COOH-FITC and G7-OH-FITC dendrimer-treated platelets express significantly less P-selectin and negatively stain for FITC, indicating no dendrimer binding. In contrast, G7-$NH_2$-FITC treated platelets express P-selectin and stain positively for FITC, suggesting dendrimer binding. The * indicates significantly different than no treatment ($p < 0.05$). The ** indicates significantly different than G6.5-COOH-FITC and G7-OH-FITC dendrimer ($p < 0.05$). Flow diagrams are from a single experiment and are representative of three independent experiments (A). The data represent the mean ± SEM of at least three independent experiments.

Individual platelet/aggregate size and adherent platelet coverage area were quantified by image analysis (ImageJ analyze particles function with the following criteria: dark background; particle size, 20-inf; particle circularity, 0.1–1.0), and results were exported to Excel (Microsoft) for statistical analysis. Data was grouped by treatment, and parameters analyzed included mean adhered platelet/aggregate size and average initial platelet binding rate (average of slopes for area covered by platelets vs time for first 90 s).

**Statistical Analysis.** Continuous variables were expressed as mean ± standard error of the mean. Pairwise comparisons were performed using a Student's *t* test. For multiple comparisons, a one-way analysis of variance (ANOVA) with a Tukey's posthoc test was used to control for error of multiple testing. Analysis for censored data was performed for lag time and time to peak. For platelet microfluidics assay, statistical analyses were performed for a given parameter and treatment by *t* tests (unpaired, two-tailed, unequal variance) on averages/slopes obtained (one per donor/treatment/parameter). A value of $p < 0.05$ was considered significant unless otherwise indicated.

## RESULTS

Characterization of native dendrimers used in this study has been recently reported.[27] The impact of FITC conjugation on dendrimer properties was minimal, as indicated by comparing native dendrimer and FITC-conjugated dendrimer characterization data for each dendrimer type. Briefly, dendrimer size does not change appreciably with FITC conjugation, as evidenced by very similar SEC elution times for both labeled and unlabeled dendrimers (Supporting Information Figure 1). Moreover, as expected, FITC-dendrimer zeta potentials shifted slightly toward neutrality when compared to those of their unconjugated counterparts. These shifts in zeta potential agree with the FITC label-dendrimer ratio measured for each dendrimer type (Supporting Information Table 1 and previously published data[27]), indicating an expected slight consumption of surface functional groups and replacement with dye chemistry.

To investigate how different dendrimer functionalizations affect human platelets, G6.5-COOH-FITC, G7-OH-FITC, and G7-$NH_2$-FITC PAMAM dendrimers (100 $\mu$g/mL, final) were added to purified platelets for 30 min and P-selectin (a marker of platelet activation) was measured using flow cytometry. Figure 1A and B shows that platelets treated with no agonist exhibited very little P-selectin expression after a 30-min incubation, while platelets treated with thrombin (0.5 U/mL, final), a protease activator receptor-1 agonist known to induce P-selectin expression, elicited significantly ($p < 0.05$) higher levels of P-selectin expression (4.9 ± 1.6% vs 94.0 ± 1.4%, respectively). Platelet P-selectin surface expression after 30 min was significantly ($p < 0.05$) increased following G7-$NH_2$-FITC dendrimer treatment (78.4 ± 11.3%), but not for either G6.5-COOH-FITC (7.6 ± 3.3%) or G7-OH-FITC (8.0 ± 4.4%) dendrimers (Figure 1A and B). To assess whether dendrimers were capable of direct platelet binding, the levels of FITC staining were concurrently examined using flow cytometry. G6.5-COOH-FITC or G7-OH-FITC dendrimer-treated platelets did not stain for FITC, indicating these dendrimers did not adhere to the platelet surface or were not internalized by the platelets. Interestingly, after a 30-min incubation, G7-$NH_2$-FITC-treated platelets were predominantly FITC-stained (92.0 ± 4.9% FITC positive), which was significantly different from the cases of no treatment and G6.5-COOH-FITC or G7-OH-FITC stimulated platelets ($p < 0.05$). This suggests that amine-terminated dendrimers are readily capable of platelet


dx.doi.org/10.1021/mp2006054 | *Mol. Pharmaceutics* 2012, 9, 1599–1611

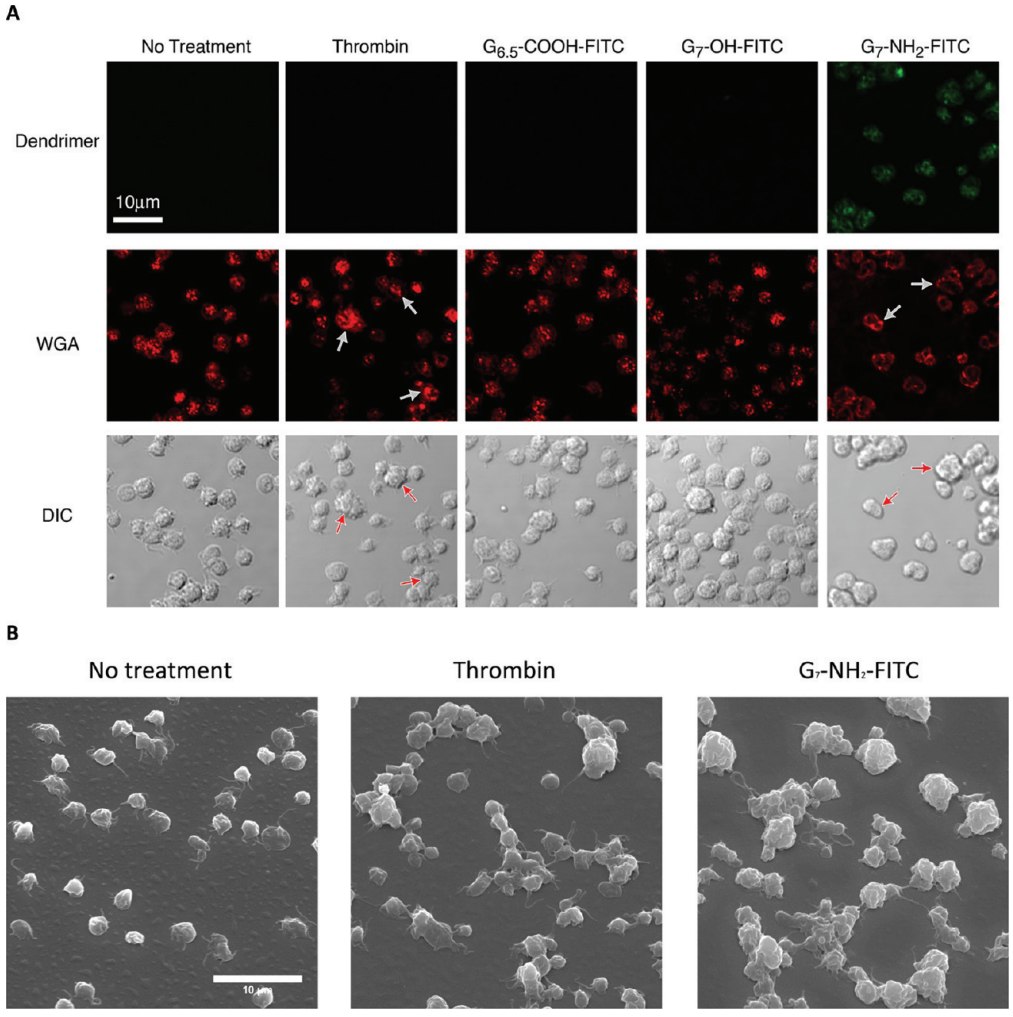


**Figure 2.** G7-$NH_2$-FITC dendrimers bind to and alter the morphology of platelets. Platelets were incubated with saline, thrombin (0.1 U/mL, final), or G6.5-COOH, G7-OH, or G7-$NH_2$-FITC dendrimer (100 $\mu$g/mL, final) for 45 min. Baseline platelets have few pseudopodia and intact granules compared to thrombin-activated platelets (A, second panel, see arrows). G6.5-COOH-FITC and G7-OH-FITC dendrimer-treated platelets have no apparent alterations in morphology, while G7-$NH_2$-FITC dendrimer treated platelets have a ruffled exterior and loss of granule morphology (see arrows) and appear green, indicating G7-$NH_2$-FITC binding to the platelet (A, right panels). Platelets were treated with saline, thrombin (0.1 U/mL, final), or G7-$NH_2$-FITC dendrimer (100 $\mu$g/mL, final) and imaged using a JEOL CarryScope SEM (B). Images were taken at 2500×, with a 20 mm working distance and a 20 kV accelerating voltage. Notice the increased number and size of platelet aggregates as well as the ruffled membrane morphology of the G7-$NH_2$ dendrimer treated platelets (B, right panel).

association (see Figure 1A and C). Next, populations of platelets staining positively for both G7-$NH_2$-FITC dendrimers and P-selectin were examined. It was determined that 92.0 ± 4.9% of platelets stained positively for dendrimer while 75.0 ± 13.1% of platelets stained positively for both dendrimer and P-selectin (shown in parts D and C, respectively, of Figure 1).

Since G7-$NH_2$ dendrimers were capable of both binding platelets and inducing platelet P-selectin expression, platelets were examined for morphological alterations produced by dendrimer treatment. Purified platelets were treated with no agonist or thrombin for 30 min, stained with WGA to observe the $\alpha$-granule morphology, and examined using confocal microscopy. Thrombin-treated platelets exhibited increased pseudopodia formation, more platelet aggregates (Figure 2A, see red arrows in the DIC row), and centralization of granules (Figure 2A, see white arrows in fluorescence row) compared to untreated platelets. G6.5-COOH-FITC- or G7-OH-FITC-treated platelets had few pseudopodia or aggregates and distinct, individual granules similar to no treatment groups (Figure 2A). In contrast with and distinct from other dendrimer-treated platelet morphologies, G7-$NH_2$-FITC-treated platelets appeared to possess ruffled exterior membranes and were found in large aggregates. Interestingly, platelets stimulated with G7-$NH_2$-FITC dendrimer had no visible pseudopodia. Furthermore, granule staining revealed general disorder along with some apparent membrane association, contrary to the granule centralization observed in thrombin-stimulated platelets. Platelet morphology was further examined by SEM, showing that, compared to no treatment and thrombin only treated platelets, G7-$NH_2$-FITC dendrimer-treated platelets were much larger in size due to aggregation. In addition, SEM imaging revealed extensive membrane ruffling of G7-$NH_2$-FITC dendrimer-treated platelets with formation of only short pseudopodia (Figure 2B). Taken together, the confocal and SEM data demonstrate that G7-$NH_2$-FITC dendrimer treatment induced dramatic alterations in platelet membrane morphology and granule structure.


dx.doi.org/10.1021/mp2006054 | *Mol. Pharmaceutics* 2012, 9, 1599–1611

Given the strong surface expression of $\alpha$-granule protein, P-selectin, on the platelet surface and the significant alterations in platelet structure and $\alpha$-granule morphology following G7-$NH_2$-FITC dendrimer treatment, additional experiments were undertaken to quantify platelet $\alpha$-granule protein release following dendrimer treatment. Specifically, RANTES and PF4—two $\alpha$-granule proteins released upon platelet activation—were assessed in dendrimer-treated whole blood. Protein release was measured at 30 min and 4 h in whole blood treated with no agonist (control) or thrombin (0.1 U/mL, final). At both time points measured, RANTES and PF4 release were significantly ($p < 0.05$) greater in thrombin-stimulated blood compared to the case of untreated platelets (Figure 3A and B). Both G6.5-COOH-FITC- and G7-OH-FITC-treated (100 $\mu$g/mL, final) platelets released RANTES and PF4 in comparable amounts to those observed for nontreated platelets. Interestingly, G7-$NH_2$-FITC dendrimer platelet treatment resulted in a significant ($p < 0.05$), time-dependent release of RANTES and PF4 compared to the cases of the other two dendrimers and untreated platelet conditions (Figure 3A and B). To ensure that this granule release was dependent on a specific dendrimer-platelet interaction, a more extensive time-dependent and dose-dependent assay was undertaken on purified platelets. Thrombin treatment of purified platelets resulted in a time-dependent release of RANTES (Figure 3C) and PF4 (data not shown), whereas untreated platelets in suspension for up to four hours released only a small amount of protein. Both G6.5-COOH-FITC- and G7-OH-FITC-treatment of platelets (100 $\mu$g/mL, final) resulted in only small amounts of RANTES and PF4 release over a 4-h period that were not significantly different from the case of nontreated platelets (Figure 3C and data not shown). However, G7-$NH_2$-FITC-treated platelet release of RANTES and PF4 occurred after only 30 min of treatment and plateaued by 1 h (Figure 3C and data not shown).

The concentration dependence of this effect was also examined. Neither G6.5-COOH-FITC nor G7-OH-FITC treatments ranging up to 500 $\mu$g/mL exerted any observable effects on RANTES or PF4 release (Figure 3D and data not shown). However, RANTES and PF4 release from G7-$NH_2$-FITC-treated platelets was significantly greater than that of G6.5-COOH-FITC and G7-OH-FITC treatments at and above 1 $\mu$g/mL, with a threshold dose of 500 ng/mL (Figure 3D and data not shown).

To assess whether dendrimer treatment altered platelet-specific functions, platelet aggregation was assessed in the presence of each dendrimer type. On the basis of impedance measurements in whole blood, stimulation with adenosine disphosphate (ADP) induced significant platelet aggregation ($p < 0.05$) compared to the case of no treatment ($10 \pm 3$ vs $0 \pm 0$ Ohms, respectively) (Figure 4A). Neither G6.5-COOH-FITC nor G7-OH-FITC induced a significant increase in platelet aggregation compared to the cases of no-treatment controls. However, G7-$NH_2$-FITC dendrimer treatment significantly increased platelet aggregation ($p < 0.05$), suggesting that platelets maintained their functional aggregation capability in response to dendrimer treatment, independent of a traditional platelet agonist (Figure 4A). Similar to aggregation trends observed in whole blood, both ADP and G7-$NH_2$-FITC dendrimer significantly ($p < 0.05$) increased the amplitude and the initial rate of platelet aggregation in PRP compared to the case of no treatment (Figure 4B and C).

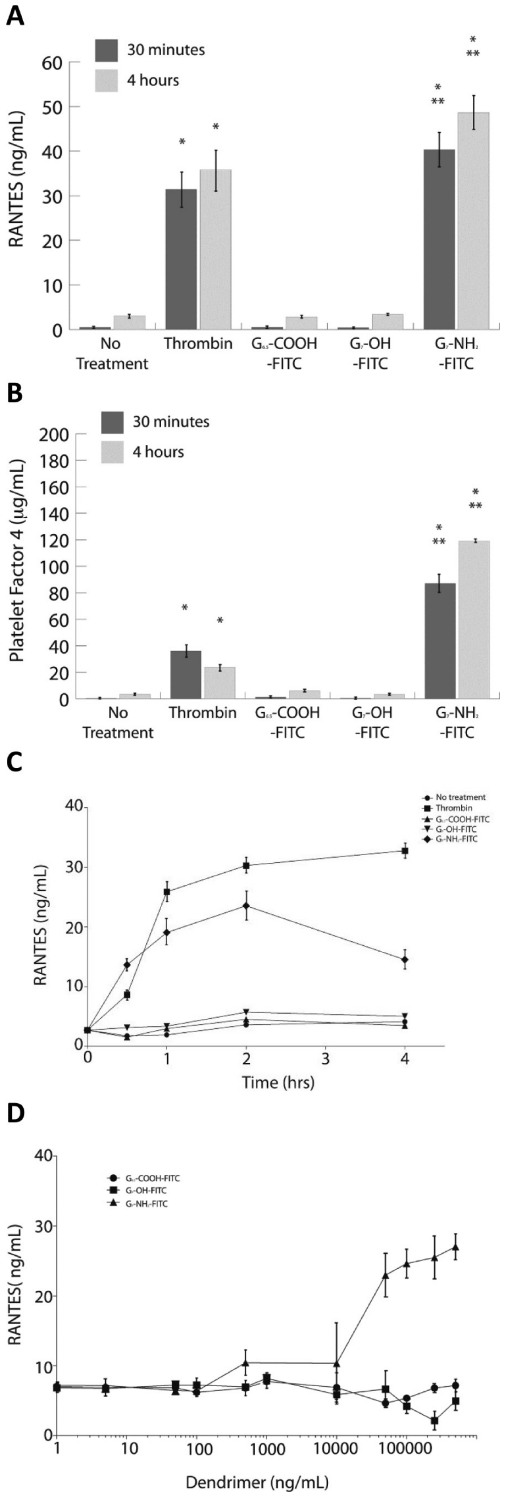


**Figure 3.** Human platelets release $\alpha$ granules contents in response to G7-$NH_2$-FITC dendrimers. Whole blood treated with G7-$NH_2$-FITC dendrimers results in significant activation of platelets based on RANTES and PF4 release after 30 min and 4 h (A and B). Purified platelets release RANTES in a dose- and time-dependent manner after treatment with G7-$NH_2$-FITC, but not G6.5-COOH-FITC or G7-$OH_2$-FITC (C and D). The * indicates a significant difference compared to the case of no treatment ($p < 0.05$). The ** indicates a significant difference compared to the cases of G6.5-COOH-FITC and G7-OH-FITC dendrimer ($p < 0.05$). The data represent the mean $\pm$ SEM of at least three independent experiments.


dx.doi.org/10.1021/mp2006054 | *Mol. Pharmaceutics* 2012, 9, 1599–1611

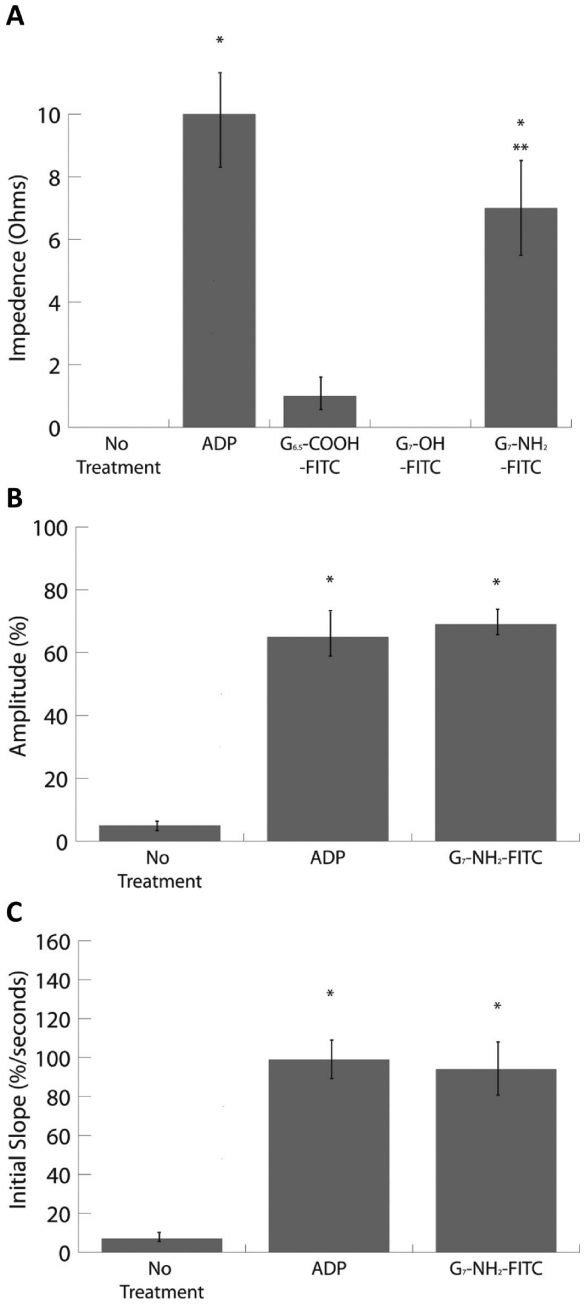


**Figure 4.** G7-$NH_2$-FITC dendrimers induce platelet aggregation. Human whole blood (A) and PRP (B and C) were treated with G6.5-COOH-FITC, G7-OH-FITC, or G7-$NH_2$-FITC (100 $\mu$g/mL, final), saline, or ADP (5 $\mu$M, final). G7-$NH_2$-FITC dendrimer treatment alone significantly increased platelet aggregation compared to no treatment (*, $p < 0.05$) and G6.5-COOH-FITC and G7-OH-FITC (**, $p < 0.05$) in whole blood. G7-$NH_2$-FITC treatment significantly increases platelet aggregation in PRP (*, $p < 0.05$) compared to the case of no treatment, as indicated by the increase in amplitude (B) and slope (C). The bars in panels A–C represent the mean ± SEM of three independent experiments.

Aside from aggregation and $\alpha$-granule secretion, another important platelet hemostatic function is to provide a specific surface to support the formation of Factor Va/Factor Xa prothrombinase complexes for the cleavage of prothrombin to active thrombin. In turn, this thrombin activates more platelets and cleaves fibrinogen to fibrin to form a fibrin clot. The combination of fibrin and activated platelets results in the formation of a stable clot to prevent bleeding. Therefore, the critical platelet function of thrombin generation was assessed for whole blood exposed to each dendrimer type. Following treatment of whole blood, thrombin generation was assessed in isolated PRP via a thrombin-specific fluorogenic substrate. Analogous G6.5-COOH-FITC- and G7-OH-FITC-treatment of whole blood had little effect on thrombin generation parameters compared to the cases of no-treatment controls (see Figure 5A and Table 1). Additionally, no dendrimer treatments elicited any observable effect on cleavage of the thrombin-specific substrate or on the fluorimetric analysis (data not shown). Surprisingly, thrombin generation in whole blood was significantly reduced uniquely for G7-$NH_2$-FITC treatment as

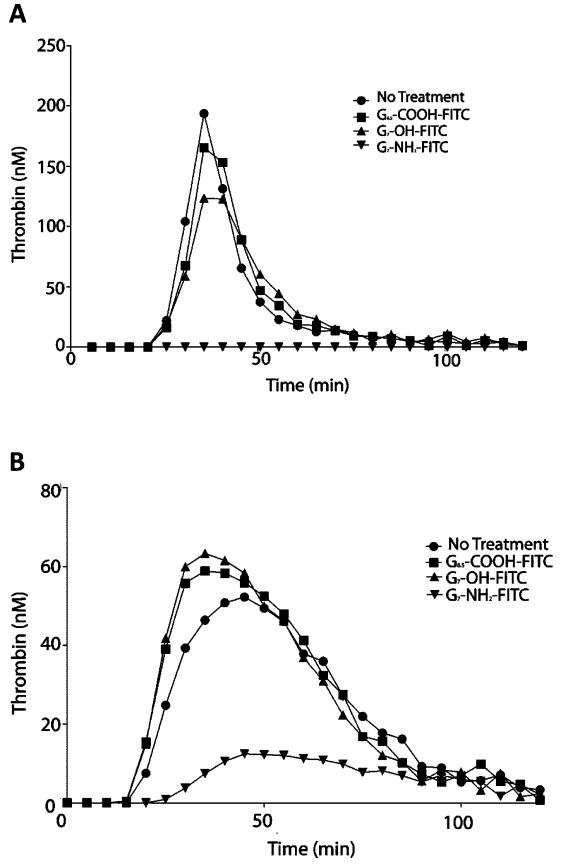


**Figure 5.** G7-$NH_2$-FITC dendrimers inhibit platelet-dependent thrombin generation in whole blood and PRP. Whole blood was treated with saline or dendrimer (100 $\mu$g/mL) for 30 min at 37 °C. After 30 min, the whole blood was centrifuged at 150*g* for 20 min and the PRP was transferred to another tube. Thrombin generation was then measured using the PRP after addition of tissue factor, $CaCl_2$, and a fluorogenic substrate. Thrombin generation was monitored with a fluorimeter for 120 min (A). G7-$NH_2$-FITC dendrimers inhibited thrombin generation in whole blood, while the G6.5-COOH-FITC and G7-OH -FITC dendrimers had little effect. Dendrimer alone had no effect on the rate of thrombin cleavage of the fluorogenic substrate or on the measurement of fluorescence (data not shown). Whole blood was centrifuged for 150*g* for 20 min, and PRP was transferred to another tube. PRP was treated with saline or dendrimer (100 $\mu$g/mL) for 30 min before thrombin generation was measured as described above. Similar to the case for whole blood, G7-$NH_2$-FITC dendrimers blunted thrombin generation in dendrimer treated PRP while G6.5-COOH-FITC and G7-OH -FITC dendrimers had no effect (B). Thrombin generation plots (A and B) depict one experiment and are representative of three independent experiments.


dx.doi.org/10.1021/mp2006054 | *Mol. Pharmaceutics* 2012, 9, 1599–1611

**Table 1. Dendrimer-Treated Whole Blood Thrombin Generation[a]**

| treatment condition | lag time (min) | peak height (nM) | time to peak (min) | rate (nM/min) | area under the curve (nM·min) |
|---|---|---|---|---|---|
| no treatment | 27.2 ± 4.2 | 112.4 ± 43.6 | 46.0 ± 8.7 | 8.3 ± 4.9 | 2449.6 ± 470.3 |
| G6.5-COOH-FITC | 27.0 ± 5.0 | 76.7 ± 34.0 | 43.8 ± 7.6 | 4.4 ± 2.4 | 2098.3 ± 595.6 |
| G7-OH-FITC | 25.3 ± 2.7 | 111.1 ± 40.1 | 46.0 ± 8.3 | 7.8 ± 3.8 | 2577.1 ± 465.0 |
| G7-$NH_2$-FITC | N.D.[b] | N.D. | N.D.[b] | N.D. | N.D.[b] |

[a]N.D. = nondetectable. [b]$p < 0.05$ compared to G6.5-COOH-FITC and G7-OH-FITC.

**Table 2. Dendrimer-Treated Platelet-Rich Plasma Thrombin Generation**

| treatment condition | lag time (min) | peak height (nM) | time to peak (min) | rate (nM/min) | area under the curve (nM·min) |
|---|---|---|---|---|---|
| no treatment | 20.0 ± 3.0 | 70.2 ± 26.4 | 41.7 ± 10.3 | 5.5 ± 3.7 | 2749.4 ± 347.4 |
| G6.5-COOH-FITC | 19.0 ± 2.1 | 65.4 ± 11.4 | 36.3 ± 3.1 | 4.1 ± 1.0 | 2924.1 ± 173.6 |
| G7-OH-FITC | 20.3 ± 2.5 | 62.3 ± 11.0 | 41.5 ± 9.5 | 4.1 ± 1.5 | 2787 ± 202.8 |
| G7-$NH_2$-FITC | 28.7 ± 2.6 | 9.6 ± 2[a] | 65.2 ± 12.1 | 0.2 ± 0.2[a] | 470.7 ± 144.2[a] |

[a]$p < 0.05$ compared to G6.5-COOH-FITC and G7-OH-FITC.

compared to all other treatments ($p < 0.05$) based on an area-under-the-curve assessment (i.e., total thrombin generation) for each treatment (Figure 5A and Table 1). Furthermore, the onset of thrombin generation (or lag time) and the time to peak thrombin concentration were significantly shortened vs untreated whole blood (control) ($p < 0.05$). The peak thrombin concentration and rate of thrombin generation were also substantially reduced but did not reach statistical significance (Figure 5A and Table 1). Again, to ensure that dendrimers acted directly on platelets and not through other blood cell mechanisms, PRP was directly isolated from whole blood and treated with dendrimer or left untreated (control). Similar to whole blood results, G6.5-COOH-FITC- and G7-OH-FITC-treated PRP had similar thrombin-generation parameters compared to nontreated control blood. G7-$NH_2$-FITC caused significant decreases in thrombin generation rate, lag time, peak height, and area under the curve compared to the cases of no treatment (control) and G6.5-COOH-FITC or G7-OH-FITC dendrimer-treated PRP ($p < 0.05$) (Figure 5B and Table 2).

*In vivo*, platelets rapidly adhere to injured vessels, activate, degranulate, and release potent agonists to help form a hemostatic plug to prevent loss of blood. To examine if dendrimer-treated platelets were capable of adhering to surfaces under physiologic flow, purified platelets were perfused through fibrinogen-coated microchannel chambers under physiologic shear conditions and platelet adhesion was quantified. Platelets stimulated with thrombin adhered to these surfaces in greater numbers and spread to a greater extent than nontreated platelets (Figure 6A DIC column and 250% DIC column). As depicted in Figure 6C and D (see also Supporting Information Figure 2A), thrombin-treated platelets also adhered at a significantly greater rate than nontreated platelets ($p < 0.05$). Non-FITC labeled G7-$NH_2$-treated platelets formed large aggregates under flow, capable of both binding to and growing from the fibrinogen-coated surface (Figure 6A and E). G7-$NH_2$-treated platelets were morphologically similar to those observed by confocal and SEM (compare Figure 6A with Figure 2). Non-FITC labeled G7-$NH_2$ dendrimer-treated platelets adhered to these surfaces at significantly faster rates and covered significantly larger areas compared to the cases of untreated platelets ($p < 0.05$) (Figure 6C and D and Supporting Information Figure 2A and Videos 1 and 2).

To examine the mechanism behind the increased rates of binding and surface coverage of cationic dendrimer-treated platelets, the role of platelet−fibrinogen binding was examined. To this end, all platelet treatment groups were pretreated with abciximab, a Fab fragment-targeting integrin $\alpha_{IIb}\beta_3$ that blocks platelet aggregation and adhesion to fibrinogen.[43] Thrombin-treated platelets pretreated with abciximab adhered at significantly lower rates and covered significantly smaller areas compared to the case of thrombin-treated platelets without abciximab treatment ($p < 0.05$) (Figure 6B−D and Supporting Information Figure 2B). Dendrimer-treated platelets pretreated with abciximab adhered to surfaces at decreased rates and covered significantly smaller areas ($p < 0.05$) compared to the case of dendrimer-stimulated platelets without abciximab pretreatment (Figure 6B−D, Supporting Information Figure 2B and Videos 3 and 4). Interestingly, cationic dendrimer treatment resulted in increased platelet aggregate size, which remained unchanged after abciximab treatment, suggesting that platelet aggregation occurs independently of $\alpha_{IIb}\beta_3$ (Figure 6E).

## DISCUSSION

Data reported here confirm and extend very recent findings on dendrimer−platelet activation effects reported *in vitro*[28] and *in vivo*.[27] This study is consistent in showing that high-generation polar neutral (hydroxyl-terminated) and anionic (carboxy-terminated) PAMAM dendrimers do not alter platelet function or morphology, while significantly, cationic (amine-terminated) G7 PAMAM dendrimers were observed to alter platelet function in both pro- and antithrombotic manners. In addition to expanding the survey of different high-generation dendrimer terminal chemistries, these data detail additional aspects of platelet biology, including platelet morphology and adhesion, and they support procoagulant surface roles that build upon and compliment previous reports focusing on dendrimer generation (size) and surface charge effects on platelet aggregation.[28] Utilizing dendrimer−FITC conjugation, the present studies demonstrate direct cationic dendrimer−platelet association. By contrast, neutral and anionic dendrimers were unable to bind platelets, while both flow cytometry and microscopic analyses demonstrated that cationic FITC-labeled dendrimers increasingly associated with platelets over time and were visually apparent on the platelet membrane (Figures 1A, 1C, and 2A), suggesting direct cationic dendrimer binding and internalization. Moreover, such potential dendrimer internalization through the platelet open canalicular system (OCS) has

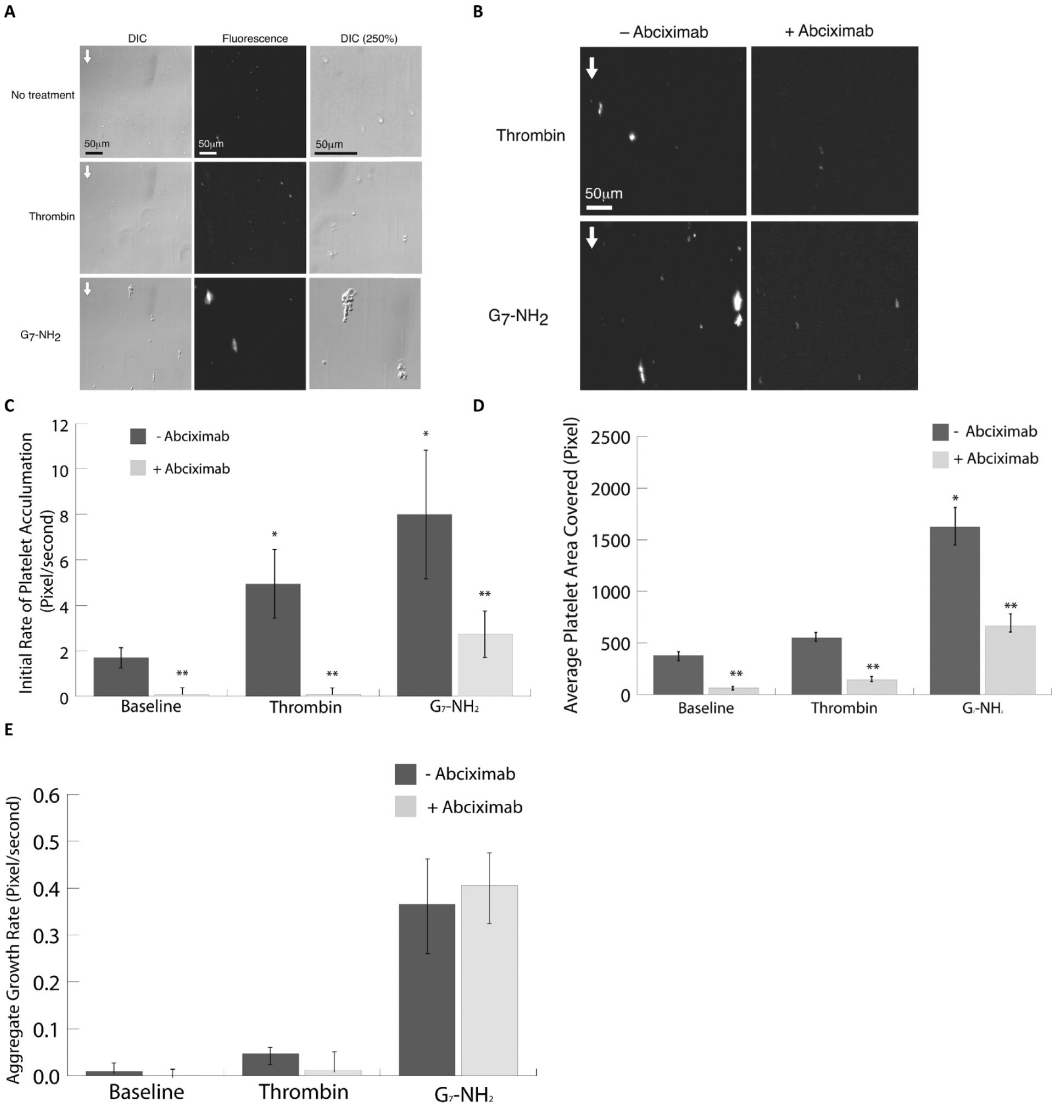


**Figure 6.** Platelets adhere faster and in greater numbers to fibrinogen under flow after G7-$NH_2$ dendrimer treatment. Platelets were left untreated or stimulated with thrombin (0.5 U/mL) or G7-$NH_2$ dendrimer (100 $\mu$g/mL) for 5 min and flowed at 200 $s^{-1}$ for 6 min over Ibidi 0.4 VI plates precoated with 0.5 mg/mL fibrinogen. In some experiments, platelets were fluorescently labeled before treatment. Images were captured in real-time using an Olympus wide-field fluorescent microscope (IX-81 inverted microscope system) using an ORCA-ER monochrome CCD camera (frame rate 1 Hz). Still images from the final frame are depicted in panel A from a single experiment, representative of 12 independent experiments. Images in panel B are still images from the final frame from one experiment, representative of six independent experiments. The flow direction is indicated by the arrow in the upper left-hand corner (A and B). The DIC image has been enlarged by 250% in the right panels to show platelet morphology. The initial rate of platelet adhesion and average area covered by platelets were significantly ($p < 0.05$) increased for dendrimer-treated platelets relative to untreated controls (C and D). In some experiments, platelets were pretreated for 1 h with abciximab (0.136 $\mu$M), a Fab fragment against $\alpha_{IIb}\beta_3$, before treatment with agonist. Abciximab-treated platelets showed reduced adhesion to fibrinogen, independent of agonist treatment (B–D). However, the aggregation behavior of platelets was not significantly different for abciximab-treated platelets stimulated with cationic dendrimer (E). The bars in panels C–E represent the mean ± SEM of at least six independent experiments. The * indicates a significant ($p < 0.05$) difference compared to the case of no treatment. The ** indicates a significant ($p < 0.05$) difference compared to the case of nonabciximab-treated platelets.

additional ramifications for platelet functional perturbations that should be explored in future studies.

Similar to previous reports,[28] this study demonstrates that cationic dendrimers induced P-selectin expression on purified platelets while neutral and anionic dendrimers had no effect on P-selectin expression (Figure 1A and B). While prior hypotheses of membrane chemomechanical disruption and permeabilization explain the observed increases in P-selectin on the platelet surface in part, the present data argue further for complete release of $\alpha$-granule contents from cationic G7 dendrimer-treated platelets as well: G7-$NH_2$-FITC dendrimer-treated platelets caused time-dependent release of $\alpha$-granule proteins RANTES and PF4 (Figure 3A–C). Moreover, even as little as 500 ng/mL of the cationic G7 dendrimer elicited secretion of these $\alpha$-granule proteins (Figure 3D). Upon activation by traditional platelet agonists such as thrombin or collagen followed by platelet–surface adherence, the $\alpha$-granule membrane fuses with the OCS, a surface-connected membrane system, or the plasma membrane to release its contents to the extracellular milieu. This activation normally results in the flattening out of the platelet with platelet organelle and granule reorganization, causing a classic "fried egg" appearance (see Figure 6A, top two DIC 250% column panels). These changes in intracellular content are mediated through the actin


dx.doi.org/10.1021/mp2006054 | *Mol. Pharmaceutics* 2012, 9, 1599–1611

cytoskeleton that directs release of the granule contents from the platelet center. In contrast to normal platelet activation, G7-$NH_2$-FITC dendrimer-treated platelets exhibited ruffled exterior cellular membranes with an enlarged, spherical gross morphology. Moreover, staining of platelet granules with WGA revealed general granular disordering with some fusion to the outer plasma membrane(s) in contrast to normal granular coalescence in the center of the platelet (Figure 2A, red-fluorescent row). These unusual alterations in both gross and granular platelet morphology support widespread actin cytoskeletal disruption. Indeed, previously published reports of highly positively charged particles contacting platelets have demonstrated changes in the actin cytoskeleton ranging from attenuation of actin polymerization to degradation of the cytoskeletal structure.[44,45] This suggests that, beyond altering plasma membrane integrity to induce platelet aggregation, G7-$NH_2$-FITC dendrimers are capable of inducing changes in the platelet cytoskeleton, resulting in release of $\alpha$-granule contents including P-selectin, RANTES, and PF4. However, this does not rule out other possibilities of direct interactions of these dendrimers with the platelet phospholipid membrane, since addition of aminated dendrimer produces visible ruffling of the platelet membrane and blunts thrombin generation that depends on phospholipid surface interactions (see below). Future studies must determine such direct interactions between dendrimer and the phospholipid membrane or the platelet cytoskeleton or both.

Aside from changes observed in platelet morphology and granule structure, G7-$NH_2$-FITC dendrimer-treated platelets exhibited dramatic changes in function compared to nontreated and thrombin-treated platelets. This has considerable consequences to blood coagulation when considering the array of proposed *in vivo* applications of dendrimers.[14] Similar to previous reports, amine-terminated dendrimers induced significant platelet aggregation in PRP.[28] This result was extended to whole blood for added physiological relevance, where addition of cationic G7 dendrimer was capable of inducing platelet aggregation, indicating that other blood cell and plasma protein components in blood have little effect on altering the cationic dendrimer−platelet interaction.

Interestingly, platelet-dependent thrombin generation was markedly inhibited by cationic G7 dendrimers in both whole blood and PRP systems, suggesting for the first time that cationic dendrimers also have a direct effect on procoagulant protein binding to platelets. Upon tissue injury, the central procoagulant enzyme, thrombin, is generated through the binding of coagulation proteins to phosphatidylserine (PS), a negatively charged phospholipid exposed on the platelet surface by activation.[46] Protein binding to the phospholipid surface is mediated through calcium cations associating with the $\gamma$-carboxyglutamic (GLA) protein domain, facilitating binding to the negatively charged PS lipid surface. Calcium associating with the GLA domain of Factor Xa facilitates Xa binding to the PS surface, resulting in the formation of the prothrombinase complex in combination with factor Va. Complete complex formation allows for cleavage of prothrombin and the generation of thrombin.[46] Cationic G7 dendrimer treatment prolonged the lag time (or onset) of thrombin generation and caused decreases in peak thrombin concentration, rate of thrombin generation, and total amount of thrombin produced. These data suggest direct dendrimer interference with enzyme reactions normally occurring on the activated platelet surface. An alternative platelet activation mechanism with dendrimers where PS is not actively involved is counterintuitive, but it supports the recent hypothesis of Dobrovolskaia et al.[28] that cationic dendrimers activate platelets in a nontraditional way. The present data suggest that cationic G7 dendrimers bind to platelet surfaces and alter the plasma membrane morphology to an extent that precludes procoagulant protein binding and prothrombinase complex formation, and that severely attenuates thrombin generation. A different explanation for this phenomenon is that cationic dendrimers induce the exposure of negatively charged PS through platelet activation, but immediately bind to those anionic phospholipids and block protein binding to the surface by virtue of concentration-dependent competition (i.e., 0.85 $\mu$M dendrimer vs 54 $\mu$M Factor X or 1.2 $\mu$M prothrombin potency) and also the cationic dendrimer polyvalent binding affinity exceeding that observed for procoagulant proteins on activated platelet surface sites ($K_d \approx 10^{-10}$).[46−48] With >500 formal positive charges present on an 8-nm diameter cationic G7 dendrimer surface, the surface area per amine group (70 Å$^2$) closely approximates the lipid headgroup density of a typical bilayer membrane, maximizing dendrimer−lipid membrane (e.g., PS) interactions, each with a contribution to the PS anionic lipid binding energy of ≈1 kcal/mol.[19] Thus, electrostatic dendrimer PS binding avidity could out-compete that of PS and Factor V with calcium. While these data suggest a direct dendrimer attenuation of platelet-mediated thrombin generation, it is also possible that amine-terminated dendrimers directly affect plasma protein procoagulant activity at platelet surfaces, altering their intrinsic ability to function as active enzymes. However, incubation of thrombin or Factor Xa (the active enzyme necessary for thrombin generation) with cationic G7 dendrimers produced no observable effect on enzyme activity (data not shown), suggesting perturbation of the plasma membrane to be a more likely explanation for the blunted thrombin response.

Of interest, Greish and co-workers[27] very recently noted a disseminated intravascular coagulation (DIC)-like condition *in vivo* resulting from intravenous cationic dendrimer injections in rodents. Superficially, this observation contradicts the present finding of decreased thrombin generation on platelet surfaces as it is thought that thrombin generation is necessary for the DIC hematologic pathology, involving extensive consumption of both platelets and coagulation proteins. However, their hypothesis that the highly positively charged dendrimer mimics the action of thrombin by independently cleaving fibrinogen to fibrin is now strengthened by the present finding of reduced thrombin generation. Therefore, a model of DIC where platelets and fibrinogen are consumed by cationic dendrimers may explain both the *in vivo* findings of Greish et al. and the present *in vitro* platelet findings.

The hypothesis of platelet consumption by high-generation cationic dendrimers is further strengthened by examining platelet adhesion under flow. Upon traditional platelet activation, the major receptor for fibrinogen, integrin $\alpha_{IIb}\beta_3$, undergoes a conformational change facilitating receptor−ligand interaction.[43] Interestingly, dendrimer-treated platelets significantly adhered to fibrinogen-coated surfaces under flow, similar to thrombin-activated platelets. However, abciximab blockage of platelet $\alpha_{IIb}\beta_3$ receptors reduced but did not eliminate some parameters of dendrimer-treated platelet adhesion, suggesting that, collectively, dendrimer-treated platelets bind to surfaces under flow by mechanisms that are potentially both fibrinogen-dependent (normal) and independent (abnormal). In these microfluidics-based experiments, abciximab at a final concen-

tration of 136 nM was preincubated with purified platelets for at least 30 min before dendrimer exposure to platelets. On the basis of reports in the literature of abciximab having a $K_d$ in platelet-rich plasma of 6.65 ± 1.45 nM,[49] it is unlikely that the abciximab would unbind from its receptor to interact with the dendrimer.

These results may seem inconsistent with previously published reports in which the platelet $\alpha_{IIb}\beta_3$ receptor blockade by abciximab did not hinder aggregation.[28] This difference in abciximab-mediated platelet observations may be explained by distinct experimental conditions: the previous platelet aggregation studies were performed under gentle stirring conditions very different from the higher shear rates of the present microfluidics assays. Furthermore, platelet aggregation measures the ability of platelets to bind to each other whereas the microfluidics assay examines platelet binding to a more physiologic substrate, in this case adsorbed fibrinogen. Superficially, the present results suggest that dendrimer-treated platelets retain functional $\alpha_{IIb}\beta_3$ receptors with abciximab treatment. However, in the present flow-based results, only platelet adhesion to fibrinogen was reduced by abciximab treatment—the adherent platelet aggregate growth rate was unchanged by abciximab addition (Figure 6E), supporting the observation by Dobrovolskaia et al.[28] that platelet aggregation occurs independently of classic mechanisms following platelet stimulation by cationic dendrimers. Interestingly, both reports present similar data for dendrimer effects on platelet membranes, showing formation of large platelet aggregates after dendrimer treatment. Therefore, it is possible that platelet aggregation after dendrimer treatment is a function of changes in membrane properties, i.e. "stickiness" in lipid membrane, and this is independent of fibrinogen binding to $\alpha_{IIb}\beta_3$ receptors.

In conclusion, the likelihood of direct cationic dendrimer interactions with platelet membrane and internal cytoskeletal structures represents a striking new mechanism for nanocarrier toxicity in blood. At circulating concentrations of ~$10^8$/mL and with intrinsically rapid (millisecond) membrane response times to both chemical and mechanical stimuli, platelets could play a significant contribution in toxicity studies of nanomaterials in blood. The new data presented here, consistent with recent reports of platelet−dendrimer interactions *in vivo* and *in vitro*, support a potent activating role for increasingly amine-terminated dendrimers and, potentially, for other cationic dendrimers in high generation, densely charged forms. This seemingly precludes their direct intravenous use in this cationic form. Additionally, extracirculatory applications of cationic dendrimers should seek to prevent transport and possible host vascular access of amine-terminated dendrimer constructs. Certainly, *in vivo* toxicities reported for PAMAM dendrimers extravascularly[21−23] provide sufficient toxicity concerns for these materials as well. Applications utilizing cationic dendrimers employed either as intravenous drug carrier precursors or platforms should provide reliable characterization for conjugation or blocking of amine terminal groups prior to blood contact. Future studies should focus on dendrimer influences on plasma proteins in general and procoagulant proteins in particular as a function of dendrimer generation and chemistry (e.g., charge density, formal charge) to further identify and understand adverse effects observed for cationic dendrimers in blood *in vivo*. Specifically, particular focus on dendrimer influences on coagulation factor activation and fibrin polymerization is needed, since dendrimer toxicity may be related to direct interactions with either blood proteins or cells, or to the modulation of complex interactions between both of these blood components.

## ■ ASSOCIATED CONTENT

### Supporting Information

Physiochemical characterization data and reaction schemes for FITC-conjugated dendrimers, additional microfluidic platelet adhesion experimental data, and microfluidic platelet adhesion videos. This material is available free of charge via the Internet at http://pubs.acs.org.

## ■ AUTHOR INFORMATION

### Corresponding Author

*Department of Pharmaceutics and Pharmaceutical Chemistry, University of Utah, Salt Lake City, UT 84112-5820, USA. E-mail: david.grainger@utah.edu. Tel: 801-581-3715. Fax: 801-581-3674.

### Author Contributions

C.F.J. and R.A.C. contributed equally to this work.

### Notes

The authors declare no competing financial interest.

## ■ ACKNOWLEDGMENTS

The authors thank D. Lim for preparing figures. Financial support was provided by NIH Grants R01DE019050, R01EB07470, R01HL065648, R01HL066277, and R01HL091754, the American Heart Association (11POST7290019), an Interdisciplinary Seed Grant from the University of Utah, the Utah Science Technology and Research (USTAR) initiative, and a University of Utah Graduate Research Fellowship.

## ■ REFERENCES

(1) Tomalia, D. A.; Fréchet, J. M. J. Discovery of dendrimers and dendritic polymers: A brief historical perspective. *J. Polym. Sci., Part A: Polym. Chem.* **2002**, *40*, 2719−2728.

(2) Radu, D. R.; Lai, C.-Y.; Jeftinija, K.; Rowe, E. W.; Jeftinija, S.; Lin, V. S. Y. A Polyamidoamine Dendrimer-Capped Mesoporous Silica Nanosphere-Based Gene Transfection Reagent. *J. Am. Chem. Soc.* **2004**, *126*, 13216−13217.

(3) Bielinska, A. U.; Yen, A.; Wu, H. L.; Zahos, K. M.; Sun, R.; Weiner, N. D.; Baker, J. R., Jr.; Roessler, B. J. Application of membrane-based dendrimer/DNA complexes for solid phase transfection in vitro and in vivo. *Biomaterials* **2000**, *21*, 877−887.

(4) Svenson, S.; Tomalia, D. A. Dendrimers in biomedical applications—reflections on the field. *Adv. Drug Delivery Rev.* **2005**, *57*, 2106−29.

(5) Esfand, R.; Tomalia, D. A. Poly(amidoamine) (PAMAM) dendrimers: from biomimicry to drug delivery and biomedical applications. *Drug Discovery Today* **2001**, *6*, 427−436.

(6) Patri, A. K.; Kukowska-Latallo, J. F.; Baker, J. R., Jr. Targeted drug delivery with dendrimers: comparison of the release kinetics of covalently conjugated drug and non-covalent drug inclusion complex. *Adv. Drug Delivery Rev.* **2005**, *57*, 2203−14.

(7) Gillies, E. R.; Frechet, J. M. Dendrimers and dendritic polymers in drug delivery. *Drug Discovery Today* **2005**, *10*, 35−43.

(8) Wilbur, D. S.; Pathare, P. M.; Hamlin, D. K.; Buhler, K. R.; Vessella, R. L. Biotin Reagents for Antibody Pretargeting. 3. Synthesis, Radioiodination, and Evaluation of Biotinylated Starburst Dendrimers. *Bioconjugate Chem.* **1998**, *9*, 813−825.

(9) Cheng, Y.; Zhao, L.; Li, Y.; Xu, T. Design of biocompatible dendrimers for cancer diagnosis and therapy: current status and future perspectives. *Chem. Soc. Rev.* **2011**, *40*, 2673−2703.

(10) Sadekar, S.; Ghandehari, H. Transepithelial transport and toxicity of PAMAM dendrimers: Implications for oral drug delivery. *Adv. Drug Delivery Rev.* **2012**, *64*, 571−588.
(11) Lai, P.-S.; Lou, P.-J.; Peng, C.-L.; Pai, C.-L.; Yen, W.-N.; Huang, M.-Y.; Young, T.-H.; Shieh, M.-J. Doxorubicin delivery by polyamidoamine dendrimer conjugation and photochemical internalization for cancer therapy. *J. Controlled Release* **2007**, *122*, 39−46.
(12) Malik, N.; Evagorou, E. G.; Duncan, R. Dendrimer-platinate: a novel approach to cancer chemotherapy. *Anticancer Drugs* **1999**, *10*, 767−76.
(13) Bhadra, D.; Bhadra, S.; Jain, S.; Jain, N. K. A PEGylated dendritic nanoparticulate carrier of fluorouracil. *Int. J. Pharm.* **2003**, *257*, 111−24.
(14) Cheng, Y.; Xu, Z.; Ma, M.; Xu, T. Dendrimers as drug carriers: Applications in different routes of drug administration. *J. Pharm. Sci.* **2008**, *97*, 123−143.
(15) Thiagarajan, G.; Ray, A.; Malugin, A.; Ghandehari, H. PAMAM-camptothecin conjugate inhibits proliferation and induces nuclear fragmentation in colorectal carcinoma cells. *Pharm. Res.* **2010**, *27*, 2307−16.
(16) Shi, X.; Lee, I.; Chen, X.; Shen, M.; Xiao, S.; Zhu, M.; Baker, J. R.; Wang, S. H. Influence of dendrimer surface charge on the bioactivity of 2-methoxyestradiol complexed with dendrimers. *Soft Matter* **2010**, *6*, 2539−2545.
(17) Domanski, D. M.; Klajnert, B.; Bryszewska, M. Influence of PAMAM dendrimers on human red blood cells. *Bioelectrochemistry* **2004**, *63*, 189−191.
(18) Li, S.-D.; Huang, L. Pharmacokinetics and Biodistribution of Nanoparticles. *Mol. Pharmaceutics* **2008**, *5*, 496−504.
(19) Zhang, Z.-Y.; Smith, B. D. High-Generation Polycationic Dendrimers Are Unusually Effective at Disrupting Anionic Vesicles: Membrane Bending Model. *Bioconjugate Chem.* **2000**, *11*, 805−814.
(20) Roberts, J. C.; Bhalgat, M. K.; Zera, R. T. Preliminary biological evaluation of polyamidoamine (PAMAM) Starburst dendrimers. *J. Biomed. Mater. Res.* **1996**, *30*, 53−65.
(21) Malik, N.; Wiwattanapatapee, R.; Klopsch, R.; Lorenz, K.; Frey, H.; Weener, J. W.; Meijer, E. W.; Paulus, W.; Duncan, R. Dendrimers: Relationship between structure and biocompatibility in vitro, and preliminary studies on the biodistribution of 125I-labelled polyamidoamine dendrimers in vivo. *J. Controlled Release* **2000**, *65*, 133−148.
(22) Heiden, T. C.; Dengler, E.; Kao, W. J.; Heideman, W.; Peterson, R. E. Developmental toxicity of low generation PAMAM dendrimers in zebrafish. *Toxicol. Appl. Pharmacol.* **2007**, *225*, 70−9.
(23) Li, C.; Liu, H.; Sun, Y.; Wang, H.; Guo, F.; Rao, S.; Deng, J.; Zhang, Y.; Miao, Y.; Guo, C.; Meng, J.; Chen, X.; Li, L.; Li, D.; Xu, H.; Wang, H.; Li, B.; Jiang, C. PAMAM Nanoparticles Promote Acute Lung Injury by Inducing Autophagic Cell Death through the Akt-TSC2-mTOR Signaling Pathway. *J. Mol. Cell Biol.* **2009**, *1*, 37−45.
(24) Wang, W.; Xiong, W.; Zhu, Y.; Xu, H.; Yang, X. Protective effect of PEGylation against poly(amidoamine) dendrimer-induced hemolysis of human red blood cells. *J. Biomed. Mater. Res. B: Appl. Biomater.* **2010**, *93*, 59−64.
(25) Jain, K.; Kesharwani, P.; Gupta, U.; Jain, N. K. Dendrimer toxicity: Let's meet the challenge. *Int. J. Pharm.* **2010**, *394*, 122−142.
(26) Ottaviani, M. F.; Daddi, R.; Brustolon, M.; Turro, N. J.; Tomalia, D. A. Structural Modifications of DMPC Vesicles upon Interaction with Poly(amidoamine) Dendrimers Studied by CW-Electron Paramagnetic Resonance and Electron Spin−Echo Techniques. *Langmuir* **1999**, *15*, 1973−1980.
(27) Greish, K.; Thiagarajan, G.; Herd, H.; Price, R.; Bauer, H.; Hubbard, D.; Burckle, A.; Sadekar, S.; Yu, T.; Anwar, A.; Ray, A.; Ghandehari, H. Size and surface charge significantly influence the toxicity of silica and dendritic nanoparticles. *Nanotoxicology* **2011**, DOI: 10.3109/17435390.2011.604442.
(28) Dobrovolskaia, M. A.; Patri, A. K.; Simak, J.; Hall, J. B.; Semberova, J.; De Paoli Lacerda, S. H.; McNeil, S. E. Nanoparticle Size and Surface Charge Determine Effects of PAMAM Dendrimers on Human Platelets in Vitro. *Mol. Pharmaceutics* **2012**, *9*, 382−393.
(29) Fischer, D.; Li, Y.; Ahlemeyer, B.; Krieglstein, J.; Kissel, T. In vitro cytotoxicity testing of polycations: influence of polymer structure on cell viability and hemolysis. *Biomaterials* **2003**, *24*, 1121−31.
(30) Hong, S.; Leroueil, P. R.; Janus, E. K.; Peters, J. L.; Kober, M. M.; Islam, M. T.; Orr, B. G.; Baker, J. R., Jr.; Banaszak Holl, M. M. Interaction of polycationic polymers with supported lipid bilayers and cells: nanoscale hole formation and enhanced membrane permeability. *Bioconjugate Chem.* **2006**, *17*, 728−34.
(31) Lee, H.; Larson, R. G. Molecular dynamics simulations of PAMAM dendrimer-induced pore formation in DPPC bilayers with a coarse-grained model. *J. Phys. Chem. B* **2006**, *110*, 18204−11.
(32) Mecke, A.; Lee, I.; Baker, J. R., Jr.; Holl, M. M.; Orr, B. G. Deformability of poly(amidoamine) dendrimers. *Eur. Phys. J. E: Soft Matter Biol. Phys.* **2004**, *14*, 7−16.
(33) Hong, S.; Bielinska, A. U.; Mecke, A.; Keszler, B.; Beals, J. L.; Shi, X.; Balogh, L.; Orr, B. G.; Baker, J. R., Jr.; Banaszak Holl, M. M. Interaction of poly(amidoamine) dendrimers with supported lipid bilayers and cells: hole formation and the relation to transport. *Bioconjugate Chem.* **2004**, *15*, 774−82.
(34) Aillon, K. L.; Xie, Y.; El-Gendy, N.; Berkland, C. J.; Forrest, M. L. Effects of nanomaterial physicochemical properties on in vivo toxicity. *Adv. Drug Delivery Rev.* **2009**, *61*, 457−66.
(35) Kitchens, K. M.; Kolhatkar, R. B.; Swaan, P. W.; Eddington, N. D.; Ghandehari, H. Transport of poly(amidoamine) dendrimers across Caco-2 cell monolayers: Influence of size, charge and fluorescent labeling. *Pharm. Res.* **2006**, *23*, 2818−26.
(36) Denis, M. M.; Tolley, N. D.; Bunting, M.; Schwertz, H.; Jiang, H.; Lindemann, S.; Yost, C. C.; Rubner, F. J.; Albertine, K. H.; Swoboda, K. J.; Fratto, C. M.; Tolley, E.; Kraiss, L. W.; McIntyre, T. M.; Zimmerman, G. A.; Weyrich, A. S. Escaping the nuclear confines: signal-dependent pre-mRNA splicing in anucleate platelets. *Cell* **2005**, *122*, 379−91.
(37) Schwertz, H.; Tolley, N. D.; Foulks, J. M.; Denis, M. M.; Risenmay, B. W.; Buerke, M.; Tilley, R. E.; Rondina, M. T.; Harris, E. M.; Kraiss, L. W.; Mackman, N.; Zimmerman, G. A.; Weyrich, A. S. Signal-dependent splicing of tissue factor pre-mRNA modulates the thrombogenicity of human platelets. *J. Exp. Med.* **2006**, *203*, 2433−40.
(38) Weyrich, A. S.; Denis, M. M.; Schwertz, H.; Tolley, N. D.; Foulks, J.; Spencer, E.; Kraiss, L. W.; Albertine, K. H.; McIntyre, T. M.; Zimmerman, G. A. mTOR-dependent synthesis of Bcl-3 controls the retraction of fibrin clots by activated human platelets. *Blood* **2007**, *109*, 1975−83.
(39) Yost, C. C.; Cody, M. J.; Harris, E. S.; Thornton, N. L.; McInturff, A. M.; Martinez, M. L.; Chandler, N. B.; Rodesch, C. K.; Albertine, K. H.; Petti, C. A.; Weyrich, A. S.; Zimmerman, G. A. Impaired neutrophil extracellular trap (NET) formation: a novel innate immune deficiency of human neonates. *Blood* **2009**, *113*, 6419−27.
(40) Weyrich, A. S.; Elstad, M. R.; McEver, R. P.; McIntyre, T. M.; Moore, K. L.; Morrissey, J. H.; Prescott, S. M.; Zimmerman, G. A. Activated platelets signal chemokine synthesis by human monocytes. *J. Clin. Invest.* **1996**, *97*, 1525−34.
(41) Weyrich, A. S.; McIntyre, T. M.; McEver, R. P.; Prescott, S. M.; Zimmerman, G. A. Monocyte tethering by P-selectin regulates monocyte chemotactic protein-1 and tumor necrosis factor-alpha secretion. Signal integration and NF-kappa B translocation. *J. Clin. Invest.* **1995**, *95*, 2297−303.
(42) Schwertz, H.; Köster, S.; Kahr, W. H.; Michetti, N.; Kraemer, B. F.; Weitz, D. A.; Blaylock, R. C.; Kraiss, L. W.; Greinacher, A.; Zimmerman, G. A.; Weyrich, A. S. Anucleate platelets generate progeny. *Blood* **2010**, *115*, 3801−9.
(43) Smyth, S.; Whiteheart, S.; Italiano, J., Jr.; Coller, B. Platelet Morphology, Biochemistry, and Function. *Williams Hematol.* **2011**, *12*, 756.
(44) Ruenraroengsak, P.; Florence, A. T. Biphasic interactions between a cationic dendrimer and actin. *J. Drug Target* **2010**, *18*, 803−11.
(45) Ellis, C. E.; Naicker, D.; Basson, K. M.; Botha, C. J.; Meintjes, R. A.; Schultz, R. A. Damage to some contractile and cytoskeleton

proteins of the sarcomere in rat neonatal cardiomyocytes after exposure to pavetamine. *Toxicon* **2010**, *55*, 1071−9.
(46) Bouchard, B. A.; Butenas, S.; Mann, K. G.; Tracy, P. B. Interactions between Platelets and the Coagulation System. *Platelets* **2007**, 1343.
(47) Tracy, P.; Peterson, J.; Nesheim, M.; McDuffie, F.; Mann, K. Interaction of Coagulation Factor V and Factor Va with Platelets. *J. Biol. Chem.* **1979**, *254*, 10354−10361.
(48) Tracy, P. B.; Nesheim, M. E.; Mann, K. G. Coordinate binding of factor Va and factor Xa to the unstimulated platelet. *J. Biol. Chem.* **1981**, *256*, 743−51.
(49) Suzuki, K.-i.; Sato, K.; Kamohara, M.; Kaku, S.; Kawasaki, T.; Yano, S.; Iizumi, Y. Comparative Studies of a Humanized Anti-glycoprotein IIb/IIIa Monoclonal Antibody, YM337, and Abciximab on in Vitro Antiplatelet Effect and Binding Properties. *Biol. Pharm. Bull.* **2002**, *25*, 1006−1012.